






RESEARCH ARTICLE

A high-impact meso-beta vortex in the Adriatic Sea

Mario Marcello Miglietta¹  | Federico Buscemi² | Stavros Dafis³  |
Alvise Papa⁴  | Alessandro Tiesi¹ | Dario Conte¹ | Silvio Davolio¹  |
Emmanouil Flaounas⁵ | Vincenzo Levizzani¹  | Richard Rotunno⁶

¹National Research Council - Institute of Atmospheric Sciences and Climate (CNR-ISAC), Bologna, Italy

²University of Bologna, Bologna, Italy

³National Observatory of Athens, Institute for Environmental Research and Sustainable Development (NOA/IERSD), Athens, Greece

⁴Centro Previsioni e Segnalazione Maree, Venice, Italy

⁵Institute of Oceanography, Hellenic Centre for Marine Research (HCMR), Athens, Greece

⁶NCAR, Boulder, Colorado, USA

Correspondence

Mario Marcello Miglietta, CNR-ISAC, corso Stati Uniti 4, 35127 Padua, Italy.
Email: m.miglietta@isac.cnr.it

Funding information

European Cooperation in Science and Technology, Grant/Award Number: COST Action CA19109 “MedCyclones”; National Infrastructures for Research and Technology S.A. (GRNET S.A.) in the Greek HPC facility - ARIS, Grant/Award Number: project adapt2CC; Tide Forecast and Early Warning Center (CPSM) - Civil Protection - Municipality of Venice, Grant/Award Number: Technical-Scientific Collaboration Agreement with CNR-ISAC

Abstract

On the evening of November 12, 2019, an exceptional high tide – the second-highest in the ranking since sea-level data have been recorded – hit the city of Venice in northern Italy and its entire lagoon, damaging a large part of its historical center. A small warm-core mesoscale cyclone, which formed in the central Adriatic Sea and intensified during its northwestward movement toward the Venice lagoon, was responsible for the event. The cyclone was preceded by intense northeasterlies (Bora) in the northern Adriatic, which turned to southeasterlies (Sirocco) and then southwesterlies after its passage. Simulations with different initialization times were carried out with the Weather Research and Forecasting (WRF) model. Simulation results show a strong sensitivity to the initial conditions, since the track (and strength) of the cyclone was determined by the exact position of an upper-level potential vorticity (PV) streamer. The factors responsible for the cyclone development and its characteristics are also investigated. The pre-existence of positive low-level cyclonic vorticity, associated with the convergence of the Sirocco and Bora winds in the central Adriatic, made the environment favorable for cyclone development. Also, the interaction between the upper-level PV anomaly and the low-level baroclinicity, created by the advection of warm, humid air associated with the Sirocco, was responsible for the cyclone’s intensification, in a manner similar to a transitory (stable) baroclinic interaction at small horizontal scales. Sensitivity experiments reveal that convection, latent heat release and sea-surface fluxes did not play a significant role, indicating that this cyclone did not show tropical-like characteristics, notwithstanding its low-level warm core. Thus, the warm-core feature appears mainly as a characteristic of the environment in which the cyclone developed rather than a consequence of diabatic processes. Lastly, the cyclone does not fall into any of the existing categories for Adriatic cyclones.

KEYWORDS

convection, cyclones, Mediterranean, mesoscale, potential vorticity, sea-surface fluxes, severe weather

Federico Buscemi Presently at 3Bmeteo

This is an open access article under the terms of the [Creative Commons Attribution-NonCommercial License](https://creativecommons.org/licenses/by-nc/4.0/), which permits use, distribution and reproduction in any medium, provided the original work is properly cited and is not used for commercial purposes.

© 2023 The Authors. *Quarterly Journal of the Royal Meteorological Society* published by John Wiley & Sons Ltd on behalf of Royal Meteorological Society.

1 | INTRODUCTION

The Mediterranean basin is one of the “climate hotspots”, where the intensity and/or frequency of intense weather events (e.g., strong winds, heavy precipitation, storm surges) is expected to increase (IPCC, 2021). The societal impact of such extremes and the possible implications of climate change have raised a renewed interest in the study of Mediterranean cyclones, both in the scientific community (Flaounas *et al.*, 2022) and by the general public. Accurate predictions are needed several days in advance to prevent or at least to mitigate potential damage to people, property, and environment. On a longer time scale, the changes in cyclone location and intensity induced by global warming have important implications for long-term policy planning.

While most cyclones affecting the Mediterranean have extratropical characteristics, subsynoptic, hybrid vortices, known as Medicanes or Mediterranean tropical-like cyclones, are occasionally observed in the Mediterranean (Emanuel, 2005; Miglietta, 2019). Although they are receiving increasing attention in the scientific literature, the mechanisms of development and intensification are not yet fully understood.

The intensification of Medicanes was shown to critically depend on sea-surface temperature (SST; Miglietta *et al.*, 2011; Pytharoulis, 2018; Noyelle *et al.*, 2019), as it affects the strength of air–sea interaction processes and thus the thermal disequilibrium responsible for deep convection. However, baroclinic instability may cooperate for their development (Flaounas *et al.*, 2021); thus, a classification was proposed, depending on the relative importance of baroclinic and diabatic processes during the mature stage (Miglietta and Rotunno, 2019; Dafis *et al.*, 2020). The SST may play a secondary role in the development of very intense extratropical cyclones, which are governed by baroclinic instability, as the recent Vaia storm (Davalio *et al.*, 2020). In all cases, upper-level dynamics control the cyclones’ evolution, determining their track and predictability (Miglietta *et al.*, 2017; Portmann *et al.*, 2020). Mediterranean cyclones are also affected by the complex topography surrounding the basin: for example, the orography may play a key role in their genesis (Buzzi and Tibaldi, 1978; Alpert *et al.*, 1999; Moscatello *et al.*, 2008a; Buzzi *et al.*, 2020), while the modulation by the rough coastline may affect their subsequent development (Rasmussen and Zick, 1987; Ricchi *et al.*, 2019).

Within the category of Mediterranean cyclones, those developing in the Adriatic Sea show specific characteristics, such as a limited extent, due to the morphology of the basin (a narrow NW-SE stretch of sea roughly 200 km wide confined between the Apennines and the Dinaric Alps). From a climatological perspective, the northern

Adriatic was identified as a region of high cyclonic activity (e.g., Campins *et al.*, 2006), or even as a prominent area for explosive deepening in the cold season (Maheras *et al.*, 2001). Horvath *et al.* (2008) identified four types of cyclones over the Adriatic Sea, each with peculiar characteristics and distinctive dynamical features:

- Type A: connected with pre-existing Genoa cyclones, they are the result of the Alpine lee cyclogenesis process (e.g., Buzzi *et al.*, 2020);
- type B: developed in situ without connections with other pre-existing cyclones; they develop either because of dynamical and thermal effects contributing to a low-level thermal anomaly in the northern Adriatic area (B-I type), or of lee cyclogenesis downwind of the central Apennines (B-II type), but with scales of motions much smaller than that in Alpine cyclogenesis;
- type AB: with mixed types A and B characteristics; this category includes cases where two cyclones coexist, in the Gulf of Genoa and in the northern Adriatic respectively (“twin” or “eyeglass” cyclones); Brzović (1999) indicates that the Adriatic twin is generated as a lee cyclone with respect to the Dinaric Alps;
- type C: cyclones of different origin moving from the Atlantic or from the western Mediterranean Sea (as in Ricchi *et al.*, 2019), apart from the Gulf of Genoa (belonging to type A).

Therefore, most cyclones reach the Adriatic after crossing the Apennines from the west; the complex orography surrounding the basin and the presence of the sea may reduce their predictability.

On November 12, 2019, a small, but very intense Adriatic cyclone contributed to a high tide, exceptional for the conditions in which it occurred (Ferrarin *et al.*, 2021), that flooded 85% of the city of Venice and affected its entire lagoon, causing major damage to the buildings. The high tide was the result of concurrent in-phase factors: the storm surge related to the meteorological forcing (the water in the northern Adriatic was pushed by the strong Sirocco and deflected westward by the Bora winds), the astronomic tide, the deep small-scale pressure minimum (inverse barometric effect), the very high sea-level values over all of the Adriatic Sea in the days before the event, and – above all – the intense southwesterlies, that pushed water toward the lagoon and generated high waves following the passage of the small-scale cyclone. The highest sea level observed in Venice was 189 cm, the second-highest ever recorded since 1872, the year in which data collection began, just 5 cm below the record reached on November 4, 1966. Unfortunately, operational weather models slightly underestimated the intensity of

the cyclone and misplaced the track by some tens of kilometers, in most cases predicting its transit to the southwest of the lagoon, and not across it as it was observed (Bianco *et al.*, 2020). Hence, considering the very specific location and topography of the affected regions and the small scale of the cyclone, current state-of-the-art models may be problematic in terms of flooding potential: even a slight misplacement may cause errors of several centimeters in the prediction of sea-level height. The specific sensitivity of the region to even the smallest errors in the cyclone track/intensity requires additional guidance involving ocean metrics (as in Ferrarin *et al.*, 2021).

The present paper aims at investigating the characteristics of the environment in which the cyclone developed, using an extensive set of surface observations and high-resolution numerical simulations. The paper is organized as follows: material and methods are reported in Section 2, synoptic analysis and surface data are described in Section 3, numerical simulation results are analyzed in Section 4, while the Discussion and Conclusions are in Section 5.

2 | MATERIALS AND METHODS

The surface data analyzed in the present study were acquired from the integrated weather–tide networks of the Italian Institute for Environmental Protection and Research (ISPRA) and of the Tide Forecast and Early Warning Center of the city of Venice (CPSM). Also, the data from two weather–tide stations (*Piattaforma Acqua Alta CNR* and *Meda Abate*), belonging to the National Research Council–Institute of Marine Sciences (CNR-ISMAR), located offshore respectively at about 15 and 40 km from the Venetian coast, are analyzed. All these stations were installed to provide a detailed representation of the meteorological/marine conditions in the North Adriatic, with the purpose of improving the predictability of high tides that frequently affect Venice (Bianco *et al.*, 2020).

A selection of weather stations was used in this work to better understand the evolution and the track of the cyclone (Figure 1). These stations were selected to represent the atmospheric conditions in Venice (Palazzo Cavalli), in different lagoon subareas (Diga Sud Lido e Faro, Chioggia Porto, Malamocco Porto), in the open sea (*Piattaforma CNR* and *Meda Abate*) as well as far away from the lagoon, on its western (Padova Meteo) and southern side (Foce Po). The real-time data and the historical series of all the 42 stations in the network are available online (www.venezia.isprambiente.it, www.comune.venezia.it/maree).



FIGURE 1 Selected weather stations in and around the Venice lagoon [Colour figure can be viewed at wileyonlinelibrary.com]

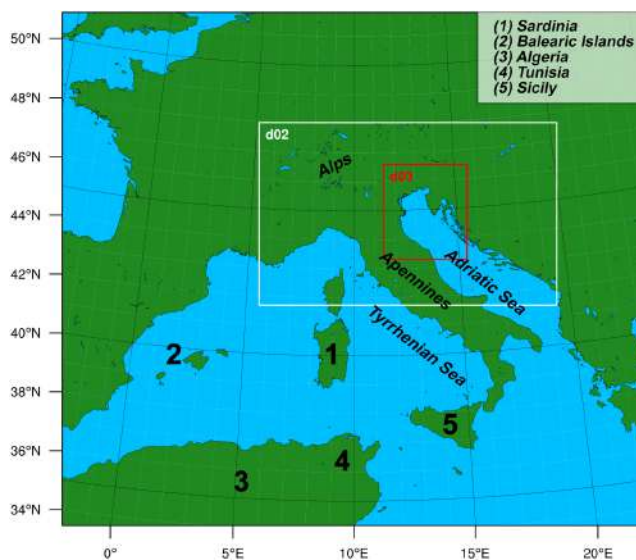


FIGURE 2 Domains used in the Weather Research and Forecasting (WRF) model simulations. The places mentioned in the text are also indicated [Colour figure can be viewed at wileyonlinelibrary.com]

Numerical simulations were performed with the WRF-ARW model, version 4.0 (Skamarock *et al.*, 2019) using three one-way nested domains (Figure 2). The grids cover respectively the western Mediterranean (grid 1, horizontal spacing 9 km, 250×220 grid points), northern and central Italy and most of the Adriatic regions (grid 2, horizontal spacing 3 km, 382×235 grid points), and the northern Adriatic Sea (grid 3, horizontal spacing 1 km, 322×364 grid points); 41 vertical levels were employed. Global Forecast System (GFS) analysis/forecasts (0.25° horizontal resolution) were used as initial and three-hourly boundary conditions respectively. The implementation in the

“control” runs includes Thompson *et al.* (2008) microphysics, the Kain–Fritsch convection scheme (activated in the two outer domains; Kain, 2004), Mlawer *et al.* (1997) long-wave radiation, Dudhia (1989) short-wave radiation, Noah land-surface model (Niu *et al.*, 2011), and the Yonsei University boundary layer (YSU; Hong *et al.*, 2006). The configuration is the one used for the simulations of an intense storm in the same region (Manzato *et al.*, 2020), with the difference that the Thompson parameterization is preferred to the WSM5 scheme following the results of preliminary sensitivity tests. Additionally, the one-way nesting option produced more realistic results than the two-way nesting configuration and was therefore employed.

3 | SYNOPTIC CONDITIONS AND SURFACE DATA

On November 10, a wide trough in the middle troposphere elongated southward from the North Sea toward the western Mediterranean (Figure 3A) and deepened due to the arrival of cold air. A surface cyclone, formed between Sardinia and the Balearic Islands at around 1200 UTC (Figure 3A), shrank and strengthened in the following 12 hr (Figure 3B). In the meantime, an upper-level pressure low appeared in the western Mediterranean. Then, its center moved over Algeria at 0000 UTC, November 11 (Figure 3B), southwest of Tunisia at 1200 UTC (Figure 3C) and approached again the Mediterranean Sea at around 0000 UTC, 12 November (Figure 3D). On November 11, the surface cyclone moved southward and gradually weakened after landing over Algeria in the evening. Another surface cyclone moved from the leeward of the Atlas Mountains, where it originated, to the southern Mediterranean at around 1200 UTC (Figure 3C), intensifying in the following 12 hr as it moved to Sicily (Figure 3D).

On November 12, the upper-level and the surface cyclones were almost aligned over the southern Tyrrhenian Sea, between Sicily, Sardinia, and Tunisia, and reached their maximum intensity (Figure 3E). The slow evolution of the depression was favored by the presence of the Azores high to the west and an anticyclone over eastern Europe (Figure 3E). Only in the evening the low weakened progressively as it moved toward the Tyrrhenian coast of southern Italy (Figure 3F). Along the northeastern border of this large-scale cyclonic circulation, a weaker, smaller-scale pressure minimum formed over the Adriatic Sea at around 1200 UTC (Figure 3E), and started moving northwestward, almost parallel to the Italian coast, reaching the Venice lagoon at around 2100 UTC (Figure 3F).

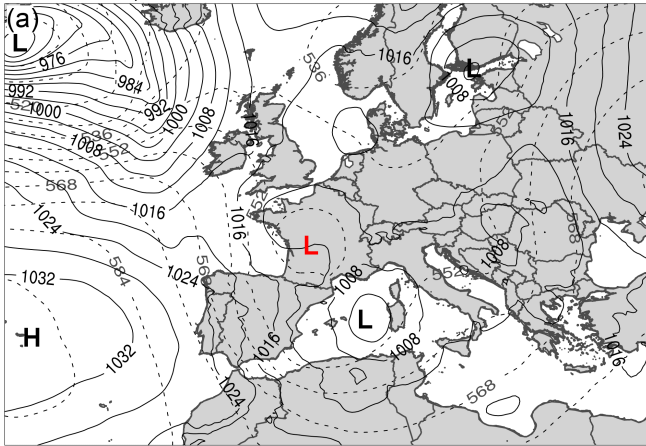
Figure 4 shows the temporal evolution of the mean sea-level pressure (mslp) at some selected stations. The rapid variation of the mslp values was associated with the passage of the small-scale cyclone, which produced a pressure drop of about 7 hPa in 3–4 hr at the stations near the cyclone track, while the recovery to the values preceding the passage of the cyclone was even faster. Because of the cyclone movement, a temporal delay of about 1.5 hr is apparent between the southern and the northernmost stations. The lowest pressure minimum (of about 987 hPa) was recorded at Piattaforma CNR, suggesting that the maximum intensity of the cyclone was probably reached over the open sea, just before it reached the lagoon.

Some indications on the precise track of the cyclone can be extracted from the overview of the observed wind fields at selected time steps (Figure 5). At 1600 UTC, a moderate Bora wind blew over the lagoon, while the cyclone was still some 100 km far south; at 1920 UTC, the approaching cyclone was revealed by easterly winds over the open sea and a progressive wind rotation in Foce Po to northwesterly and then to southwesterly at 2005 UTC, the latter associated also with an intensification of the wind speed. Thus, at 2005 UTC the observations indicate that the cyclone center was located on the north side of the Po Delta, close to the Adriatic coast. The wind barbs at 2040 and 2055 UTC identify a small-scale cyclonic circulation entering the lagoon from its southern part, where wind directions reversed over a distance of a few km; also, while intense southeasterlies blew over the open sea, sustained northeasterlies were still affecting the northern side of the lagoon.

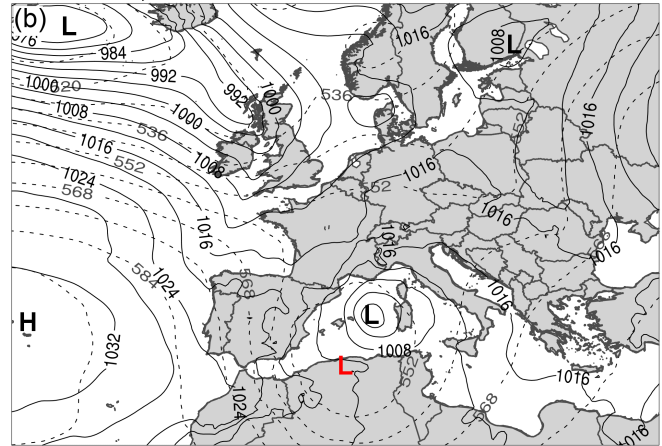
Lastly, at 2125 UTC, as the cyclone moved inland, the wind rotated to southwesterly in the southern part of the lagoon and over the open sea, attaining its maximum intensity in response to the strong pressure gradient on the rear of the cyclone. Many stations in and around the lagoon (Figure 6) recorded fierce winds up to 29 m s^{-1} in “Diga Sud Lido e Faro” station. The strong southwesterlies pushed the water toward the northern side of the lagoon, contributing to the extreme high tide. Following these considerations, the cyclone center is estimated to have remained close to the Adriatic coast along its entire track, landing just north of Chioggia (Figure 1).

Figure 7 compares the evolution of different surface parameters at two selected stations respectively over the open sea (Piattaforma CNR) and in Venice (Palazzo Cavalli). The measurements show an increase in the 2-m air and dewpoint temperature as the cyclone approached the stations: in Piattaforma CNR, a sudden increase of more than 4 K in 10 min preceded the arrival of the pressure minimum by about 50 min. During the next hour, the air temperature remained almost constant, decreasing rapidly

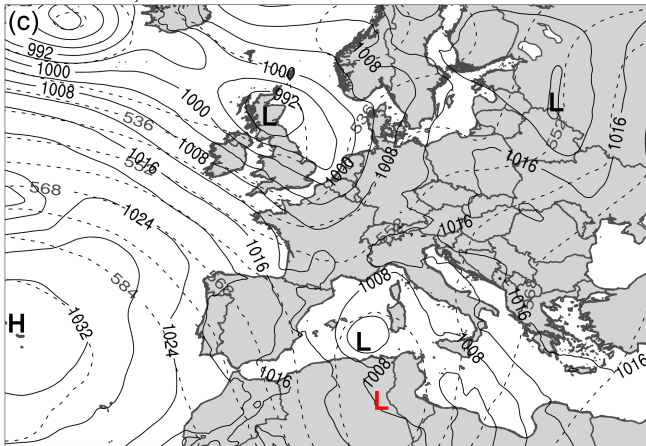
2019-11-10, 1200 UTC



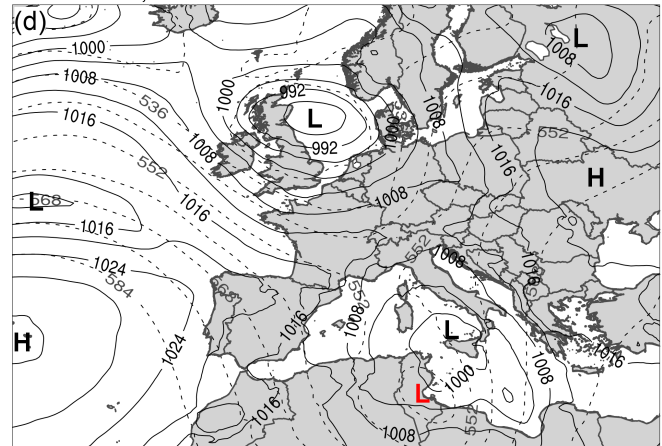
2019-11-11, 0000 UTC



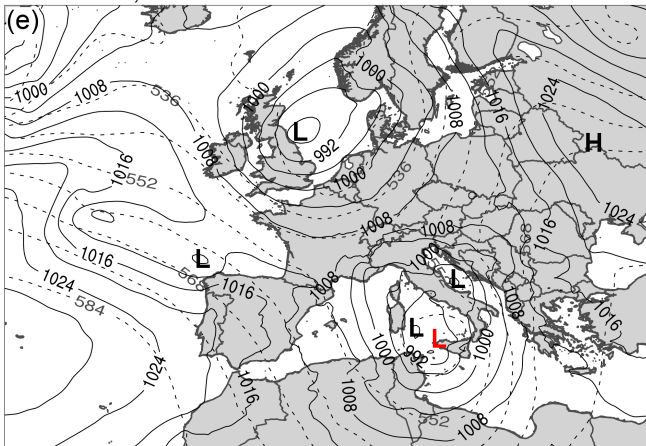
2019-11-11, 1200 UTC



2019-11-12, 0000 UTC



2019-11-12, 1200 UTC



2019-11-12, 2100 UTC

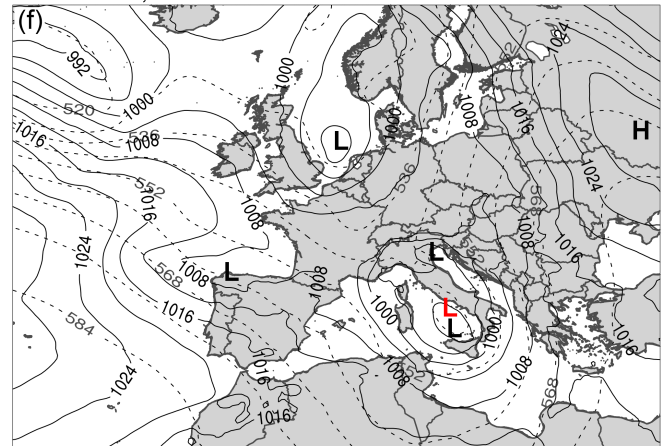


FIGURE 3 ERA5 reanalysis of 500 hPa geopotential height (dashed lines, in gpdam) and mean sea level pressure (mslp) (dark lines, in hPa) at (a) 1200 UTC, November 10, 2019; (b) 0000 UTC and (c) 1200 UTC, November 11, 2019; (d) 0000 UTC, (e) 1200 UTC, and (f) 2100 UTC, November 12, 2019. The red “L” denotes the position of the upper-level low [Colour figure can be viewed at [wileyonlinelibrary.com](https://onlinelibrary.wiley.com/doi/10.1002/qj.4432)]

15 min after the passage of the minimum. The increase in dew point temperature was smaller, determining a reduction in relative humidity from saturation to 80%. At the Venice station a similar evolution was observed, but with

a delay of 30 min; however, the temperature increase was less steep and mainly distributed in two distinct phases. After the passage of the cyclone, the environmental parameters went back to the previous values.

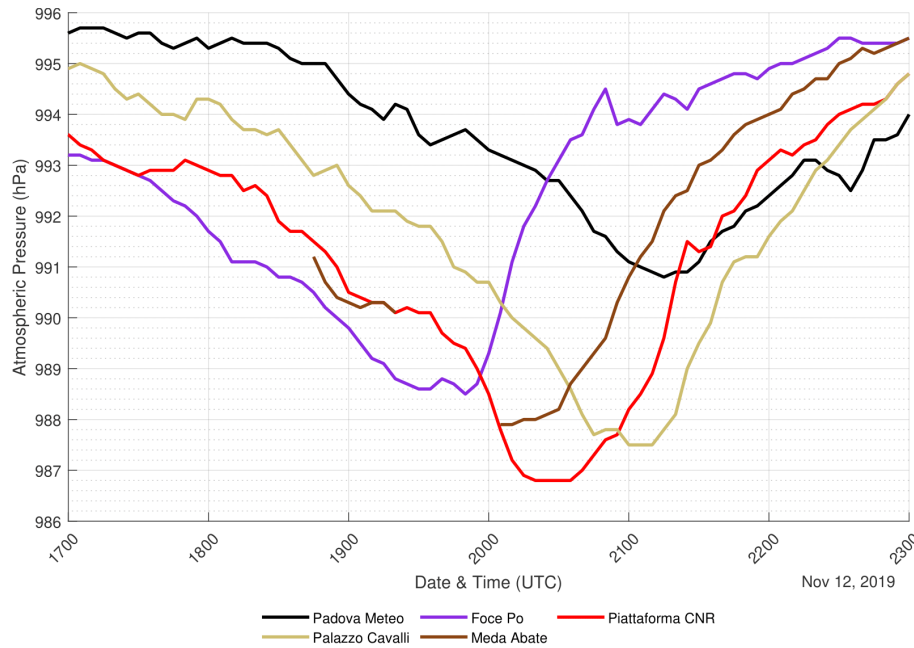


FIGURE 4 Mean sea level pressure (mslp) (hPa) between 1700 UTC and 2300 UTC, November 12, 2019 in selected surface stations [Colour figure can be viewed at [wileyonlinelibrary.com](https://onlinelibrary.wiley.com/doi/10.1002/qj.4432)]

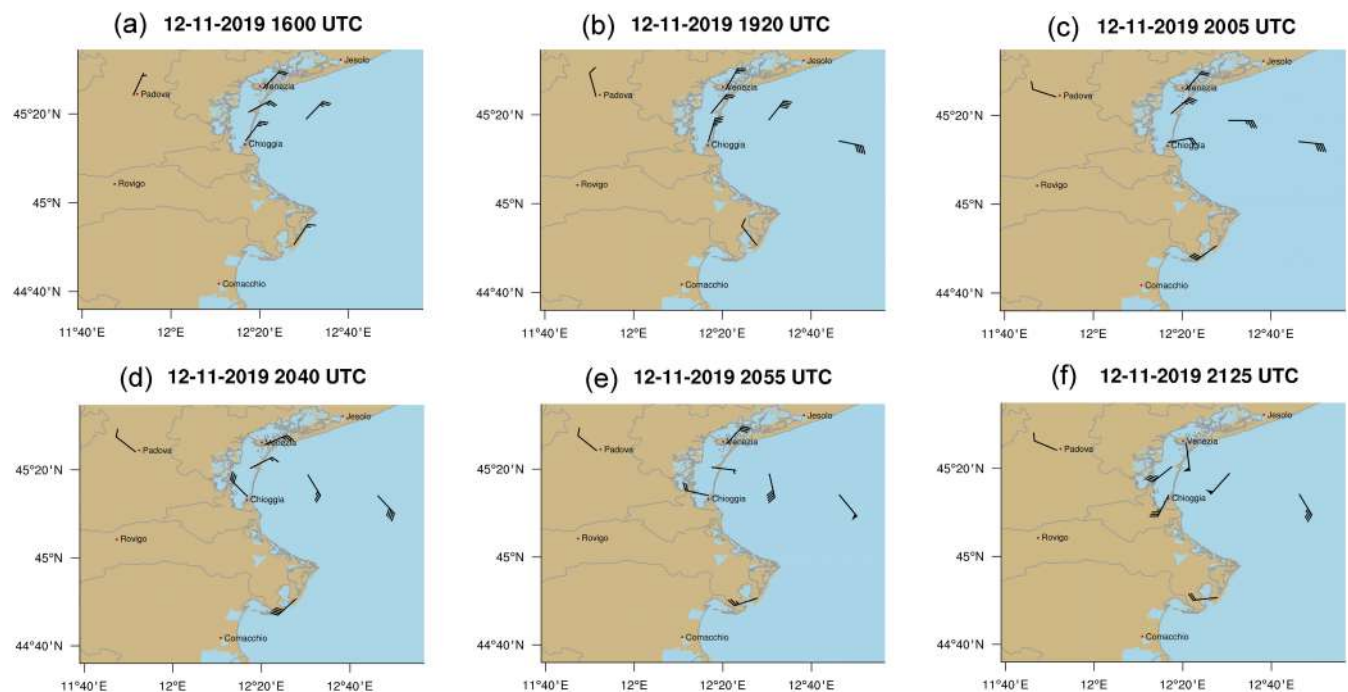


FIGURE 5 Wind barbs in selected surface stations at six significant time steps during the cyclone transit. [Colour figure can be viewed at [wileyonlinelibrary.com](https://onlinelibrary.wiley.com/doi/10.1002/qj.4432)]

In conclusion, the presence of a low-level warm core (Figure 7), the rapid change in wind speed near the center (Figure 6), and the appearance of a cloud-free center in the visible satellite image (not shown) suggest a possible tropical-like nature of the cyclone, although the horizontal extent appears smaller than that recorded in any previous case (cf. Miglietta *et al.*, 2013). However, for a Medicanne, which is mainly driven by air–sea interaction and latent

heat release due to convection around the cyclone, the warm core is expected to be nearly symmetric and close to center. Figure 7 shows that in the present case the warm core preceded the arrival of the pressure minimum by about 1 hr and ended abruptly after its passage. Hence, considering these contrasting features, numerical simulations were performed to better clarify the nature (baroclinic vs tropical-like) of the cyclone.

FIGURE 6 Five-min average wind speed peaks (top) and direction (bottom) recorded in selected weather stations [Colour figure can be viewed at [wileyonlinelibrary.com](https://onlinelibrary.wiley.com)]

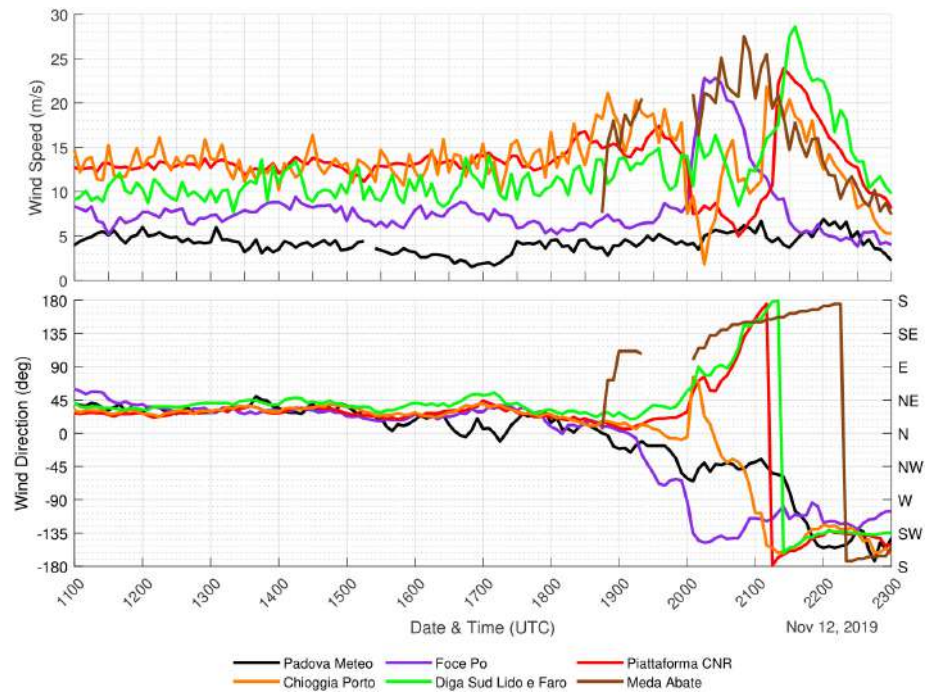
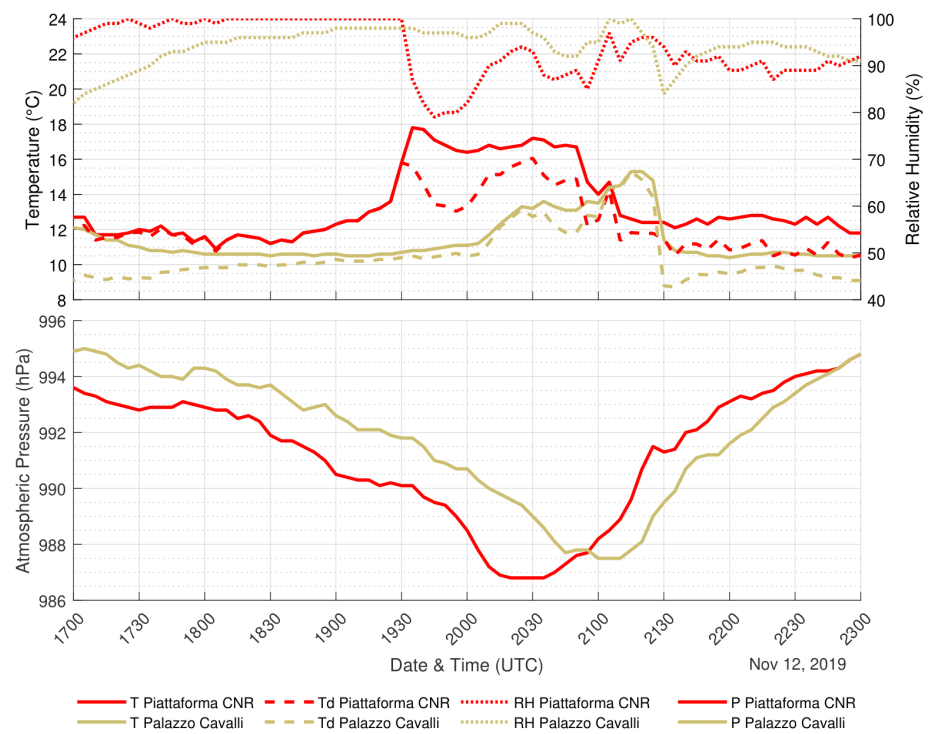


FIGURE 7 Upper panel: Air temperature (T , solid line), dew point temperature (T_d , wide dashed line) and relative humidity (RH, narrow dashed line). Bottom panel: sea level pressure. The fields are shown at Piattaforma CNR and Palazzo Cavalli stations [Colour figure can be viewed at [wileyonlinelibrary.com](https://onlinelibrary.wiley.com)]



4 | NUMERICAL SIMULATIONS

4.1 | Preliminary results

To investigate the predictability of the event and to understand the physical mechanisms responsible for the development of the cyclone, numerical simulations were carried out with the WRF-ARW model. A first intercomparison

was performed among three model simulations starting at different initial times, that is, 1200 UTC, November 11, 0000 and 1200 UTC, November 12 (hereafter named as run 1,112, 1,200, and 1,212 respectively). As described below, the cyclone track and intensity differed significantly among the simulations.

Figure 8A shows the time evolution of mslp simulated at the grid point closest to the Palazzo Cavalli weather

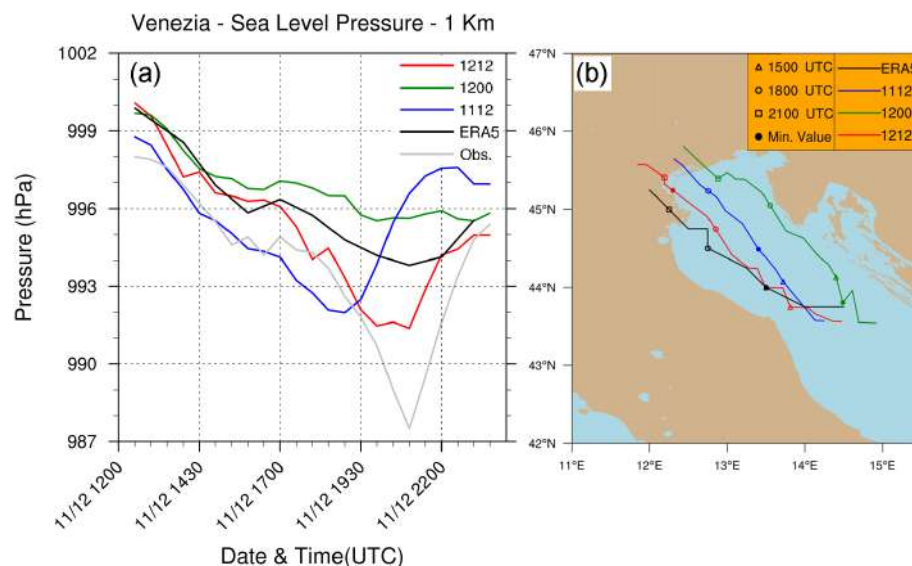


FIGURE 8 Mean sea level pressure (mslp) at Venice in control runs and observed value (Palazzo Cavalli weather station) – grid 3 (left); cyclone track – grid 1 (right). The tracks in grid 1 are shown since they are smoother than in the inner grid [Colour figure can be viewed at [wileyonlinelibrary.com](https://onlinelibrary.wiley.com/doi/10.1002/qj.4432)]

station (Figure 1). Only run 1,212 is able to correctly reproduce the intensification of the cyclone in the late evening, although it underestimates the minimum by 4 hPa; in contrast, run 1,112 precedes its occurrence by a few hours, while ERA5 reanalysis, and to a greater degree run 1,200, strongly underestimate its deepening. Simulations performed with other models (BOLAM, COSMO-LAMI, ECMWF IFS) have similarly showed large uncertainties in reproducing the observed cyclone evolution (Bianco *et al.*, 2020).

Similarly, the cyclone track (i.e., the line connecting the minimum mslp locations at different times) significantly differs among the numerical experiments. Figure 8B shows that only run 1,212 correctly predicts the landfall on the southern side of the lagoon; the ERA-5 track is positioned to the west, and, consequently, precedes the observed landfall (over the Po Delta) by a few hours; run 1,200 puts the cyclone track too far east, while run 1,112 reproduces an intermediate track, which crosses the north side of the Venice lagoon. The limited predictability of the cyclone track can be also inferred from the ECMWF IFS runs issued 1–4 days earlier, which simulate an early landfall near the Po Delta only partially corrected in the later run initialized at 0000 UTC, November 12 (Cavaleri *et al.*, 2020).

Another relevant aspect emerging from the simulations is the extremely weak sensitivity to grid spacing. For all experiments, the outputs on the three domains are nearly identical to each other; this result is somewhat unexpected considering the small dimensions of the cyclone, which should be better resolved at higher resolution. The archive of the operational runs performed with two limited area models developed at CNR-ISAC, that is, BOLAM (Davolio *et al.*, 2020; 8.3 km grid spacing) and MOLOCH (Malguzzi *et al.*, 2006; Trini Castelli *et al.*, 2020;

1.25 km grid spacing), available at <https://www.isac.cnr.it/dinamica/projects/forecasts/>, shows similar results, as the strength of the cyclone simulated with the coarser model (hydrostatic, convection parameterized) appears very similar or even slightly more intense than that obtained with the finer-scale model (non-hydrostatic, convection permitting). Similarly, Hallerstig *et al.* (2021) found that for four polar lows the difference in performance between the 9-km and 5-km versions of the ECMWF model, either with parameterized or with explicit convection, was relatively small, especially for the two cyclones with baroclinic characteristics (their Figure 8). Following the hypothesis of Cioni *et al.* (2018) for a Mediterranean tropical-like cyclone, that “simulations performed with a grid spacing larger than 5 km are not able to correctly resolve the deep convection” and that convection “weakening or even absence compromises the forecast of the cyclone evolution over time”, and given the simulation results described above, we speculate that latent heat release in convective cells does not play a relevant role for the present case study. This conclusion is also supported by the negligible differences in cyclone track and depth among simulations using a treatment of convection other than the control run (i.e., explicit convection either in the two inner grids or in all three grids; not shown).

Lastly, further numerical experiments were performed to test different model parameterization schemes and domains (not shown). Sensitivity to these characteristics is significantly weaker than that due to initial/boundary conditions (as discussed above) but is still responsible for changes in the cyclone strength and track. These changes, although small from a meteorological point of view, may yield problematic guidance in terms of flooding potential, having a strong effect on the simulation of wave height and surge (Ferrarin *et al.*, 2021). In fact, the impact of the latter

in a small-scale basin such as the Venice lagoon is strongly dependent on even minimal variations in meteorological parameters and requires additional guidance in terms of ocean metrics.

4.2 | Insight into the development mechanism

The atmospheric conditions in which the cyclone developed are analyzed here using the run 1,212 to better understand the physical mechanisms responsible for its intensification. As discussed in Section 3, the cyclone appeared in the central Adriatic, in the lee of the Apennines, in the afternoon of November 12, and then moved counterclockwise driven by the larger-scale cyclonic circulation centered over the Tyrrhenian Sea. As a result of the latter, the Mistral developed over the western Mediterranean basin, while intense Sirocco winds affected the southern and central Adriatic Sea, with greater intensity on the eastern (Croatian) coast (Figure 9). Meanwhile, the northern Adriatic was still under the influence of northeasterly (Bora) wind, so that, at the border between the two circulations (Sirocco and Bora), strong low-level cyclonic vorticity (an ingredient favorable to the formation of Mediterranean cyclones; Cavicchia *et al.*, 2014) developed over the central Adriatic before the appearance of the cyclone. Later, the Sirocco progressively strengthened and entered the northern Adriatic, so that the developing cyclone was advected northward by the southeasterly steering flow.

Figure 10 shows the 2D frontogenesis function (Petterssen, 1936), defined as the rate of change over time of the horizontal potential temperature gradient:

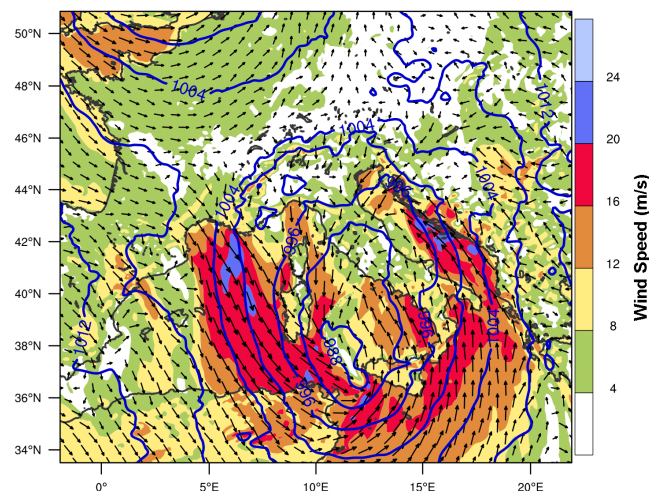


FIGURE 9 Mean sea level pressure (mslp) (hPa) and wind speed (m/s) at 1400 UTC, November 12, 2019 (grid 1) [Colour figure can be viewed at [wileyonlinelibrary.com](https://onlinelibrary.wiley.com)]

$F = \frac{d}{dt} |\nabla_p \theta|$; here it is calculated at 950 hPa (the highest values are observed in the layer 1,000–950 hPa) from the large-scale GFS data used to force the numerical simulations. As the warm environment in which the cyclone developed moved northward, the horizontal thermal gradient in the baroclinic zone on the northern side of the cyclone progressively increased.

The change in the thermal environment surrounding the cyclone can be identified in Figure 11. A baroclinic zone appeared at the upper level in the afternoon, associated with the approach of cold air from the south that produced an increase in the thermal gradient in the layer 600–300 hPa (green contours). Conversely, a core of low-level warm air in the layer 1,000–700 hPa (red contours) surrounded the mslp minimum, remaining confined around it at 2000 UTC. Meanwhile, a tongue of low-level warm air moved from the central to the northern Adriatic coast in about six hours, as indicated by the northward movement of the 290 K isotherm at 1000 hPa (blue contours).

Consequently, in the low levels the low- θ_e air in the northern Adriatic was progressively replaced by a high- θ_e air tongue carried by the Sirocco from the southern Adriatic Sea. A comparison of the low-level θ_e at different times in the three panels of Figure 12 reveals the warm tongue progressively weakened as the air moved northward, due to the mixing with the surrounding low- θ_e air, which was transported over the northern Adriatic initially by the Bora and later by southwesterly winds from the Po valley on the rear side of the cyclone. In fact, the counterclockwise circulation associated with the small-scale cyclone advected the high- θ_e air to its front side, preceding the arrival of its center. Meanwhile, on its rear, the outflow of cold/dry air from the eastern Po valley, generated by the evaporative cooling of the precipitation at the foot of the Apennines (as discussed in section 3.2 of Ferrarin *et al.*, 2021), interrupted the supply of warm and moist air from the south (Figure 12C).

Therefore, the cyclone pressure center was not aligned with the low-level θ_e maximum, but lagged instead at its back, in an environment of strong horizontal thermal gradient, in accordance with the observed temporal shift between the arrival of warm air and the pressure minimum (Figure 7). Considering the distribution and temporal evolution of θ_e , one may speculate that the warm air was not a consequence of diabatic processes associated with the cyclone (i.e., generated by the latent heat released by convection), but rather a characteristic of the environment in which the cyclone formed. This is consistent with the analysis of the simulations in Section 4.1, where convection was inferred to play only a marginal role in the development of the cyclone, and with the sensitivity experiments in Section 4.3.

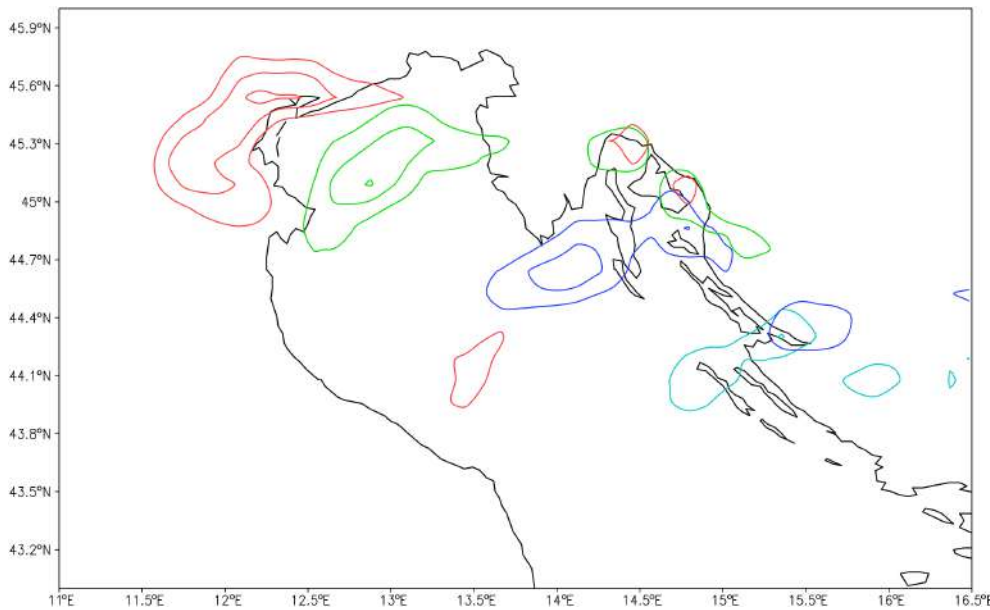


FIGURE 10 950 hPa frontogenesis function at 1200 UTC (cyan), 1500 UTC (blue), 1800 UTC (green), 2100 UTC (red). The contours refer to 1, 2, 3 $\text{K} \cdot (\text{km})^{-1} \cdot \text{h}^{-1}$ (the outer the contour, the lower the value). The figure is based on GFS data [Colour figure can be viewed at [wileyonlinelibrary.com](https://onlinelibrary.wiley.com/doi/10.1002/qj.4432)]

To further illustrate this point, Figure 13 reports the vertical velocity at different levels (850, 700, 500 hPa) one hour before the cyclone reached its pressure minimum (2000 UTC). Only scattered and shallow convection was simulated, mainly confined below 5-km altitude. The most intense ascending motions appear in the Alpine area, due to the southerly flow over the orography (Figure 13B), and near the Venice lagoon (Figure 13C), at the northern and western end of the high- θ_e air tongue, where the warm air was raised above the pre-existent cold low-level air (in the region, the latter often acts as an obstacle to the incoming moist and warm southerly flow; Davolio *et al.*, 2016). Thus, the numerical simulations appear consistent with the sporadic lightning activity observed on the northwestern side of the cyclone before its landfall (https://www.blitzortung.org/en/historical_maps.php?map=10).

Finally, the contribution of the upper-level atmospheric features to the development of the cyclone is analyzed in Figure 14, which shows the 300-hPa potential vorticity (PV) at 2000 UTC for the three runs. In both runs 1,112 (Figure 14A) and 1,212 (Figure 14C), the cyclone was positioned near an upper-level PV anomaly: in the first case, a secondary PV maximum was reproduced on the north side of the lagoon (the main streamer was positioned to the west), while in the latter, an intense PV streamer approached its southwestern part. In contrast, run 1,200 (Figure 14B) reproduced the PV anomaly inland, apparently unrelated to the position of the cyclone. Therefore, there are significant differences among the simulations in terms of intensity and exact position of the PV streamer. These results suggest that in run 1,212 its position just above the observed cyclone location was critical to correctly reproduce the cyclone track: the PV anomaly

was in correspondence with the left exit of a jet stream that surrounded the synoptic cyclone (not shown), thus its location was favorable to the cyclone's intensification. Hence, we suppose that the upper-level dynamics played an important role for the evolution of the cyclone, and that were also fundamental for the correct prediction of the event, consistent with the results recently obtained for an intense Mediterranean cyclone (Portmann *et al.*, 2020), although the scales involved here are much smaller. The role of the upper-level PV streamer and of its interaction with the warm and moist air advected in the low levels will be further discussed in the next subsection.

4.3 | Sensitivity experiments

To further investigate the mechanisms responsible for the intensification of the cyclone, a series of sensitivity experiments was undertaken. As in run 1,212 (control run), the GFS analysis and forecasts initialized at 1200 UTC on November 12 were used as initial and boundary conditions. Only one domain (9-km horizontal spacing) was employed, considering the marginal effect of the resolution on the simulation results.

The sensitivity to different physical processes was explored in five numerical experiments:

1. NoSFFX: Full physics, but surface fluxes turned off;
2. NoLH: full physics, but latent heat release turned off;
3. OnlyPBL: microphysics, radiation, and cumulus schemes turned off;
4. NoPhys: surface fluxes, latent heat release, and all physics parameterization schemes turned off;

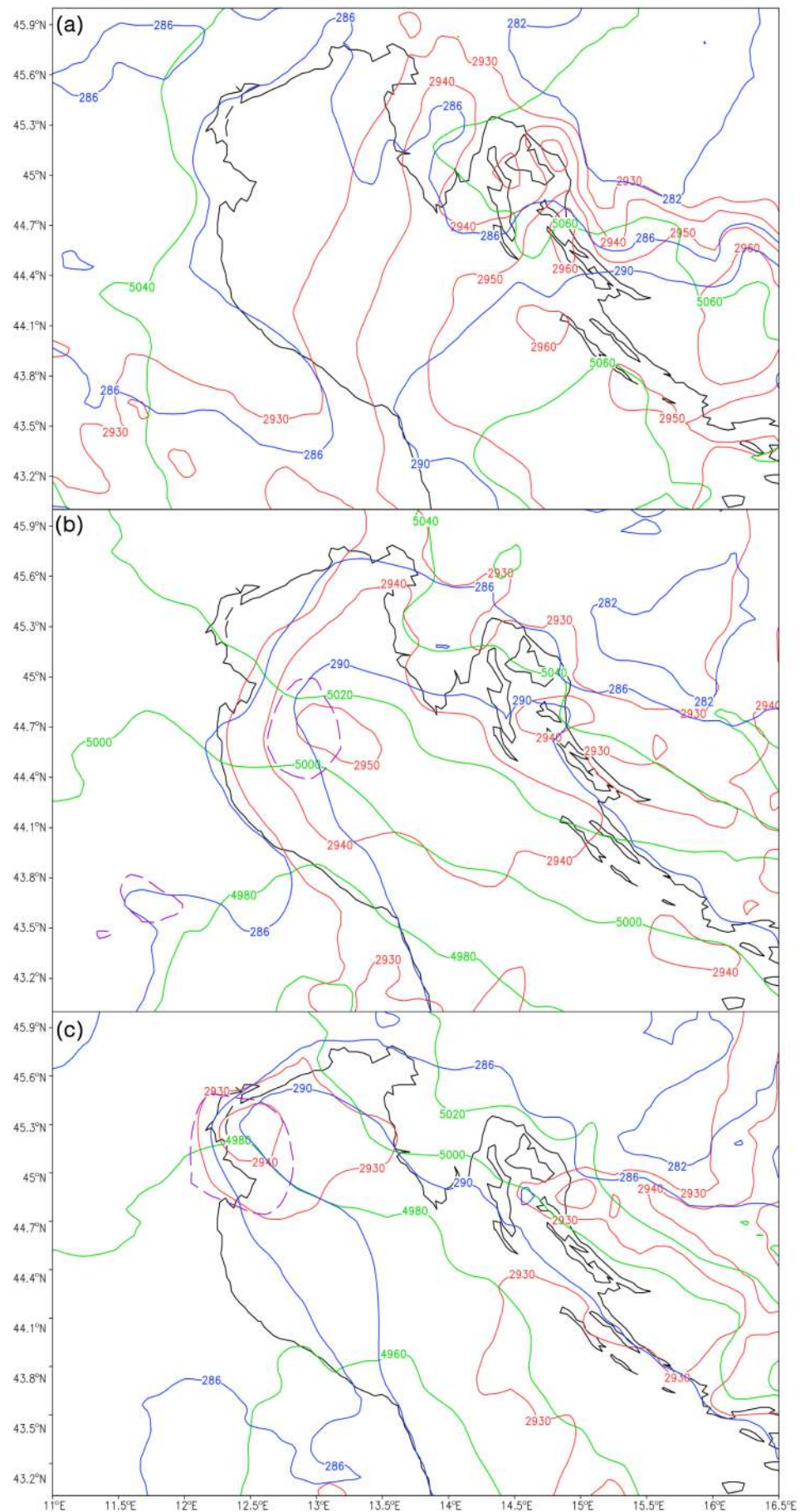


FIGURE 11 Weather Research and Forecasting (WRF) model simulation, Grid 1: 1000 hPa temperature (blue contours; values: 282, 286, 290 K), 700–1,000 hPa depth (red contours; values: 2930, 2,940, 2,950, 2,960 gpm), 600–300 hPa depth (green contours; values: 4960, 4,980, 5,000, 5,020, 5,040, 5,060 gpm), at 1400 UTC (A, top), 1800 UTC (B, middle), 2000 UTC (C, bottom). The isobar of 991.5 hPa is also shown (purple dashed contours) at 1800 UTC and 2000 UTC to identify the cyclone location [Colour figure can be viewed at [wileyonlinelibrary.com](https://onlinelibrary.wiley.com/terms-and-conditions)]

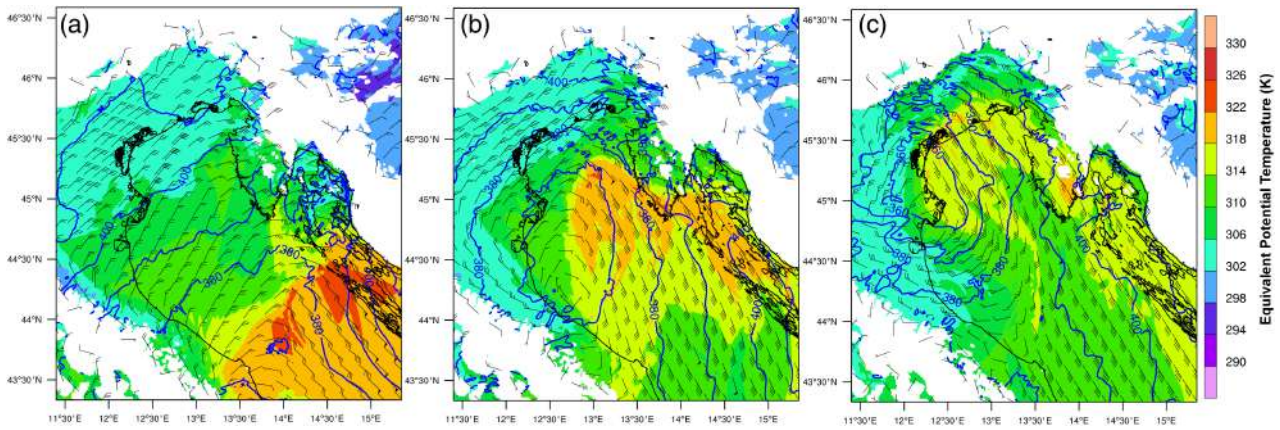


FIGURE 12 950 hPa equivalent potential temperature (K) and wind at 1400 UTC (A), 1800 UTC (B) and 2000 UTC (C), November 12, 2019 (grid 3) [Colour figure can be viewed at [wileyonlinelibrary.com](https://onlinelibrary.wiley.com)]

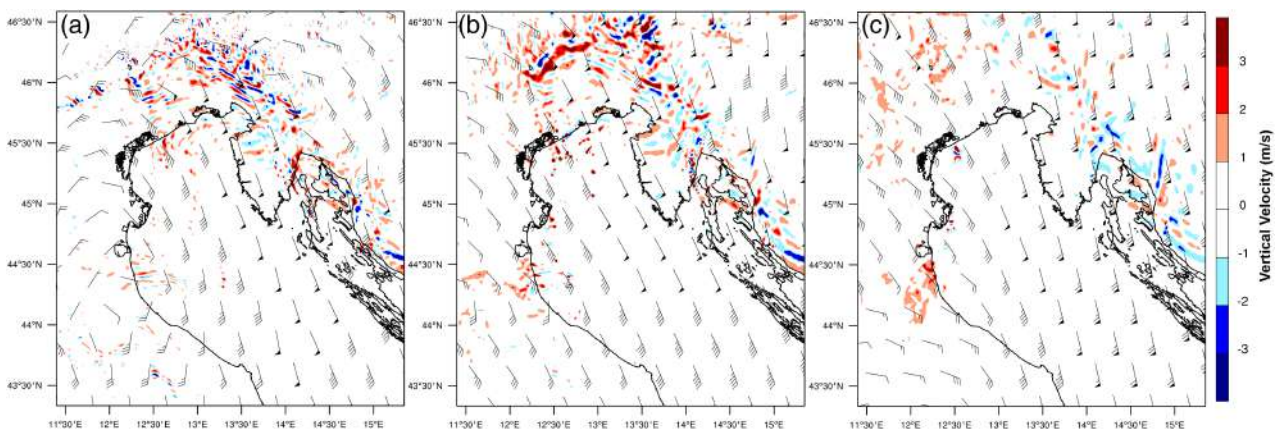


FIGURE 13 Vertical velocity (colors) and horizontal wind (barbs) at 1900 UTC, November 12, 2019, at 850 hPa (A), 700 hPa (B) and 500 hPa (C) (grid 3) [Colour figure can be viewed at [wileyonlinelibrary.com](https://onlinelibrary.wiley.com)]

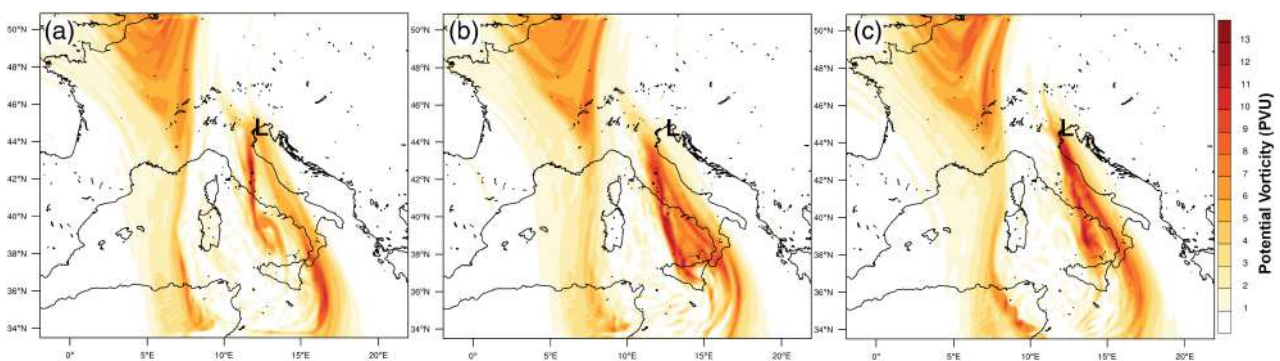


FIGURE 14 300 hPa PV (PVU) at 2000 UTC, November 12, 2019, in run 1,112 (A), 1,200 (B) and 1,212 (C) (grid 1). The bolded “L” denotes the position of the mean sea level pressure (mslp) minimum [Colour figure can be viewed at [wileyonlinelibrary.com](https://onlinelibrary.wiley.com)]

5. NoPhysNoTopo: as NoPhys, but with terrain height equal to 1 m everywhere over land in the domain.

In all experiments 1–4, the track and landfall time were very close to those of the control run, so that the changes

in the outputs can be considered as an effect of the physics and cannot be attributed to changes in the track.

In the NoSFFX run, the absence of surface fluxes caused a weakening of the small-scale minimum by about 2 hPa (Figure 15A). However, the cyclone can

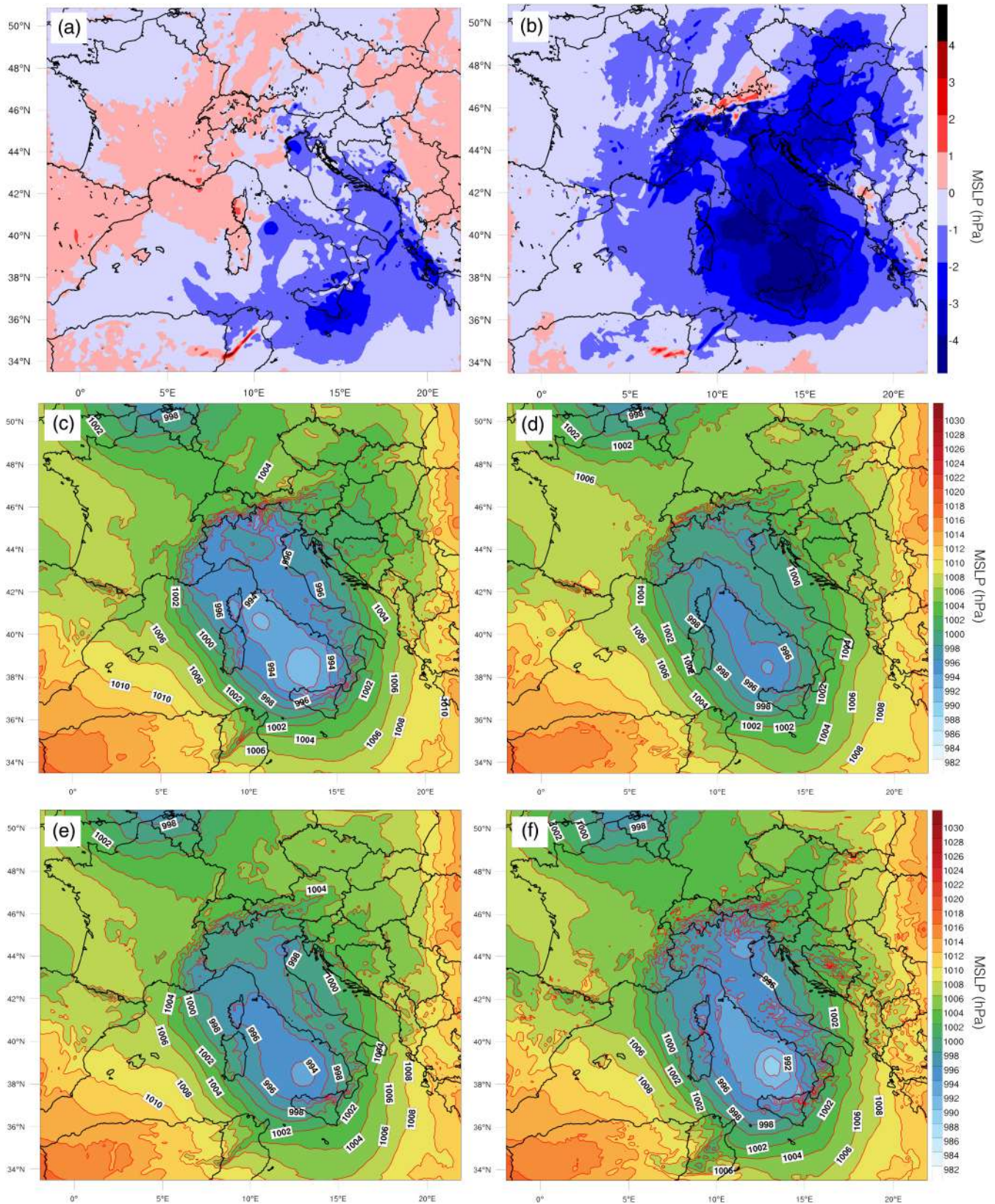


FIGURE 15 Mean sea level pressure (mslp) difference (colors; hPa) between the control run and (A) the NoSFFX run, (B) the NoLH run; mean sea level pressure (mslp) (colors and contours; hPa) in (C) NoSFFX run, (D) NoLH run, (E) Only PBL run, and (F) NoPhys run. Figures are shown at 2130 UTC, November 12, 2019 [Colour figure can be viewed at [wileyonlinelibrary.com](https://onlinelibrary.wiley.com)]

still be identified near Venice (Figure 15C), showing that the air–sea interaction processes, while participating in the cyclone intensification, were not fundamental for its occurrence and persistence. Likewise, surface fluxes only marginally affected the large-scale cyclone over the Tyrrhenian Sea.

In the NoLH run, the absence of latent heat release produced a substantial increase in mslp in all the areas affected by the large-scale cyclonic circulation covering the central Mediterranean basin, the strongest increase (greater than 4 hPa) being near the center of the Tyrrhenian cyclone (Figure 15B). The Adriatic cyclone was only marginally affected, since the variation in mslp was only 1 hPa greater than in the surrounding areas, so that closed isobars can still be clearly identified around the mslp minimum (Figure 15D). Hence, the NoLH run confirms that convection had a secondary effect on the small-scale cyclone. The two sensitivity experiments NoSFFX and NoLH indicate that the cyclone would persist even after removing air–sea interaction and convection, although the latter explain part of its intensification. In order to apply the “factor separation” technique (Stein and Alpert, 1993) and estimate the interaction of the two terms, an additional sensitivity experiment has been undertaken by removing simultaneously the surface fluxes and latent heat release, showing results very close to that of the NoLH run. This means that the small-scale cyclone had distinctive characteristics from Mediterranean tropical-like cyclones, which,

conversely, are mostly sustained by diabatic processes and a strong feedback between air–sea interaction and convection.

Even in the OnlyPBL run (microphysics, convection, and radiation switched off; boundary layer processes active) and in the NoPhys run (all parameterization schemes, sea-surface fluxes and latent heat release switched off), the cyclone, albeit weaker, can still be identified near the Venice lagoon (Figure 15E,F respectively). Apparently, physics changed the cyclone evolution, but it was not required for its existence.

Lastly, a simulation without physics (as in the NoPhys run) and with flat orography (NoPhysNoTopo run) was performed. Even in this case, a closed minimum formed near the northern Adriatic Italian coasts, on the northern side of the trough axis extending from the large-scale minimum. The absence of orography apparently modified the location of the cyclone, which in this run was located inland, instead on the lee side of the Apennines, as observed. However, the presence of a small-scale minimum even without physics and orography (Figure 16A) suggests that the large-scale forcing was the main driver for the development of the cyclone.

Using a diagnostic module implemented into the WRF model for the PV budget (Flaounas *et al.*, 2021), PV was calculated and decomposed into one conserved and several non-conserved partitions at each model time step. All these PV partitions are treated by the model

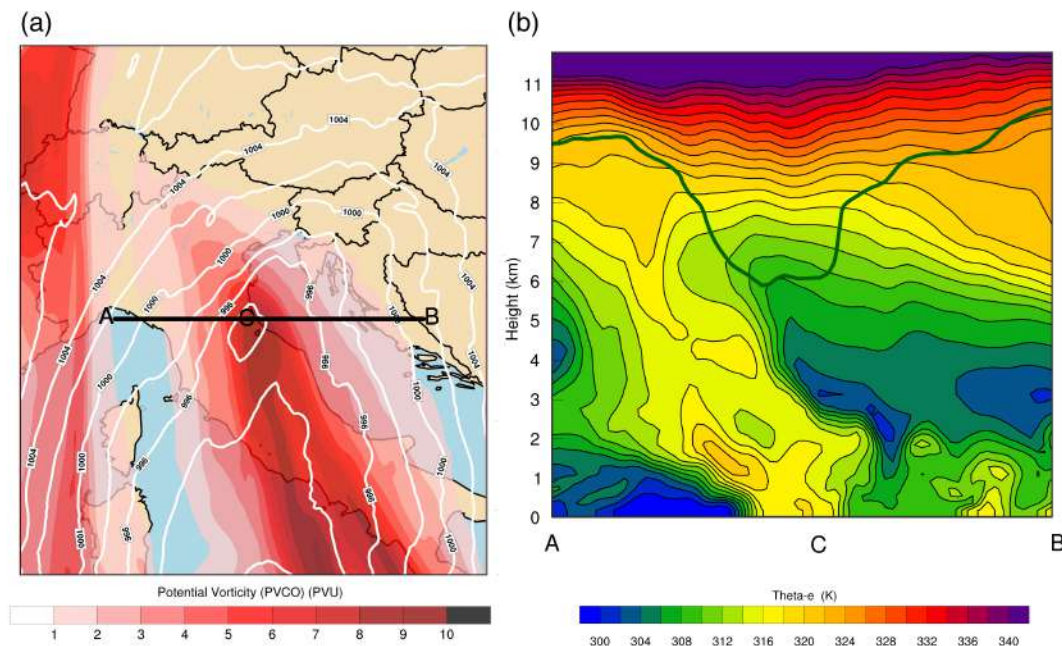


FIGURE 16 (A) Mean sea level pressure (mslp) (white contours; hPa) and adiabatic, conserved part of the potential vorticity (PV) anomaly PVCO (colors; PVU) at 300 hPa; (B) vertical cross section across the cyclone center of equivalent potential temperature (K; colors) and dynamic tropopause (PV = 2 PVU; green line). Figures are shown at 1900 UTC, November 12, 2019, and refer to the NoPhysNoTopo run. The position of the cross section in (B) is shown in (A) [Colour figure can be viewed at wileyonlinelibrary.com]

as scalars, subject to advection. The adiabatic, conserved PV tracer (PVCO) represents the contribution of the large-scale flow and is only subject to advection. Conversely, non-conserved PV partitions are also subject to accumulations of gains/losses of PV, and derive from the net temperature and momentum forcings associated with the physical parameterization schemes. Overall, six non-conserved PV tracers are used, deriving from: latent heat release (microphysics and convection parameterizations); turbulent fluxes of temperature (boundary layer); atmospheric warming and cooling (short-wave and long-wave radiation), and a momentum acceleration term (boundary layer). Details on how these terms are calculated can be found in Flaounas *et al.* (2021).

Positive values of PVCO appear close to the cyclone center before and around the time of its intensification (Figure 16A). Figure 16B clarifies the interaction of the upper-level PV anomaly, associated with the lowering of the dynamic tropopause, with the baroclinicity at the side of the low-level warm tongue (i.e., high values of equivalent potential temperature), which was shifted westward with respect to the control run because of the suppression of the orography. Low values (below 10 K) of the coupling index (Bosart and Lackmann, 1995), around the area of cyclone development (central Adriatic) at 1200 UTC and over the region of its maximum intensification (Venice lagoon) at 1800 UTC, indicate the presence of conditions favorable to the interaction between positive upper-tropospheric and lower-tropospheric PV anomalies around the cyclone location (not shown).

Also, these results suggest some analogies with the mechanism theoretically described in Rotunno and Fanfani (1989), their Figure 2, that is, a transitory (stable) baroclinic interaction. In this kind of development, a surface cyclone forms and deepens when a pre-existing upper-level trough encounters a low-level baroclinic zone (Petterssen's Type-B extratropical cyclones; Petterssen and Smebye, 1971) even for wavelengths shorter than that required for instability, since the system is capable of extracting energy from the mean flow.

4.4 | Surface pressure tendency

To further investigate the atmospheric processes that contributed to the deepening of the cyclone, we used an additional diagnostic, that is, the surface pressure p_{sfc} tendency equation (Fink *et al.*, 2012):

$$\frac{\partial p_{sfc}}{\partial t} = DF + ITT + EP + RES \quad (1)$$

where: $DF = \rho_{sfc} \frac{\partial \phi_{p_2}}{\partial t}$ is the contribution due to the changes of the geopotential height ϕ at p_2 (ρ_{sfc} : air density at the surface), $EP = g(E - P)$ is the contribution of the change in water vapor mass due to evaporation E and precipitation P (g : gravitational acceleration), $ITT = \rho_{sfc} R_d \int_{sfc}^{p_2} \frac{\partial T_v}{\partial t} d \ln p$ is the vertically integrated virtual temperature T_v tendency (R_d : gas constant for dry air), and RES is the residual term due to numerical discretization. The equation was applied to a vertical column from the surface to the upper boundary $p_2 = 50$ hPa as in Fita and Flaounas (2018).

ITT can be further decomposed into:

$$ITT = TADV + VMT + DIAB + RES, \quad (2)$$

where: $TADV = \rho_{sfc} R_d \int_{sfc}^{p_2} -\vec{v} \cdot \nabla_p T_v d \ln p$ is the contribution of the horizontal virtual temperature advection (\vec{v} is the horizontal wind), $VMT = \rho_{sfc} R_d \int_{sfc}^{p_2} \left(\frac{R_d T_v}{c_p p} - \frac{\partial T_v}{\partial p} \right) \omega d \ln p$ is the contribution of the vertical motion (c_p is the specific heat capacity at constant pressure p ; ω the vertical wind component in isobaric coordinates), $DIAB = \rho_{sfc} R_d \int_{sfc}^{p_2} \frac{T_v Q}{c_p T} d \ln p = TBL + THD + TLW + TSW$ represents the rate of change of temperature due to diabatic processes calculated by the WRF physical parameterizations (Q is the diabatic heating, TBL planetary boundary layer-related processes, THD microphysics and convective processes including latent heat release, TLW long-wave radiation, and TSW short-wave radiation).

Integration was performed every 30 min over a circle of 100-km radius centered at the position of the surface cyclone; hence, due to the progressively smaller cyclone size, the area-average p_{sfc} remained nearly constant or slightly increased (rates less than 1 hPa 1 hr⁻¹), although the minimum mslp progressively decreased as the cyclone approached Venice. All terms with time tendencies were calculated as area- or volume-averaged changes in 30 min, while the instantaneous terms TADV and VMT were computed by integration over the volume and then averaged over the time interval.

Figure 17A shows the different contributions to the equation and the total pressure tendency. The contribution of evaporation/precipitation EP appears marginal, while the geopotential change DF at the upper boundary is mainly responsible for a decrease of p_{sfc} at the time the PV streamer wrapped around the cyclone and the dynamic tropopause lowered just above its center (from about 1830 to 2000 UTC in the control run).

Figure 17B shows the different contributions to the ITT term. Although a comprehensive interpretation is not possible due to the non-negligible residual, some considerations can be drawn:

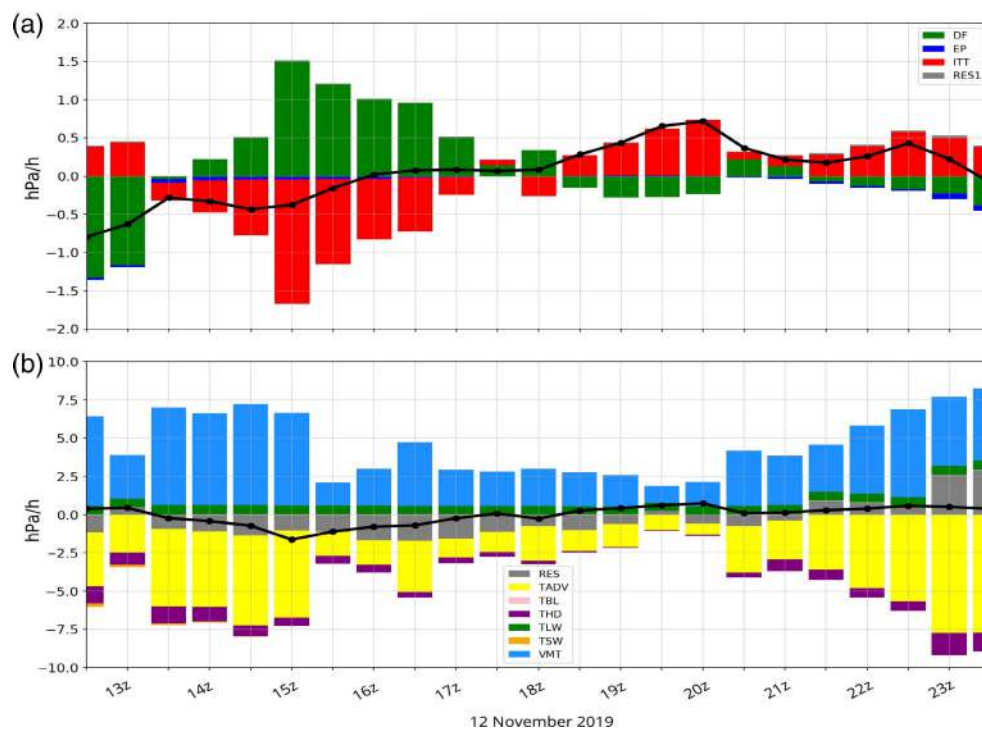


FIGURE 17 (A) Surface pressure tendency (black line), decomposed into: contributions by 50 hPa geopotential height (DF), integrated column temperature (ITT), evaporation and rainfall (EP), and a residual term (RES). (B) Integrated temperature term (ITT; black line), decomposed into contributions by: horizontal advection (TADV), vertical motion (VMT), and diabatic heating processes due to boundary layer (TBL), microphysics and convection (THD), long-wave (TLW), and short-wave radiation (TSW). Model outputs are reported every 30 min, while pressure tendency is shown in $\text{hPa} \cdot \text{h}^{-1}$ [Colour figure can be viewed at wileyonlinelibrary.com]

- THD is very small during the cyclone intensification, confirming that microphysical processes (e.g., latent heat release) play a marginal role in its evolution;
- TADV is always negative, which is indicative of warm advection associated with the northward transport of warm air from the southern Mediterranean;
- TSW and TBL provide almost no contribution;
- TLW represents a small positive contribution (diabatic cooling);
- VMT is always positive and can be attributed to the large-scale ascent associated with the lifting of the warm air advected from the south over the cold air pre-existent in the low levels in the northern Adriatic Sea.

These results appear consistent with those emerging from the sensitivity experiments and in the previous subsections and are indicative of the high influence of synoptic-scale dynamics on the cyclone evolution.

5 | DISCUSSION AND CONCLUSIONS

The present paper describes the unusual Mediterranean cyclone that affected the Venice lagoon on November 12, 2019. Although the skill of the real-time weather forecasts was generally acceptable from a meteorological perspective (cyclone track missed by few tens of km and depth underestimated by few hPa), the fine details necessary

for impact applications were missed; consequently, the operational prediction of the storm surge peak was underestimated by some tens of cm, misrepresenting the severity of the tide that unexpectedly flooded most of the town, with dramatic consequences in terms of costs and impact to human activities. Here, the event is re-analyzed from a meteorological perspective, to understand the mechanism(s) of development of the small-scale cyclone that was responsible for the extreme tide.

Numerical simulations performed with the WRF model, using three nested domains, show a strong sensitivity to the initial conditions: over the three full-physics simulations starting at different initial times, only the one starting closer to the occurrence of the cyclone shows an excellent agreement with the observed track, although it slightly underestimates the strength of the cyclone. The high-resolution inner domain, which explicitly resolves convection, does not improve the simulation results compared to the coarsest domain that uses parameterized convection; a similar behavior was reported in the numerical simulations performed for the same case with other meteorological models. This unexpected result is a consequence of the scattered and shallow convection simulated by the model, which has a negligible impact on the intensification of the cyclone.

The strong PV advection in the upper levels, combined with a pre-existing relative vorticity maximum (associated with the confluence of the Sirocco with the Bora wind) and the advection of warm and moist air in the lower levels, appear as the main factors responsible for the strong

intensification of the cyclone in the northern Adriatic. In particular, the interaction of the upper-level (adiabatic) PV anomaly with the low-level baroclinic zone recalls a transitory (stable) baroclinic interaction at small horizontal scales.

The cyclone analyzed in the present work shows peculiar characteristics, which do not exactly fit into any of the categories proposed in Horvath *et al.* (2008) for Adriatic cyclones. Like category B-II cyclones, it has a small scale and originates downwind of the central Apennines; however, its movement along the Adriatic coast and its strong intensity differ from the typical characteristics of B-II cyclones (see Figure 3 in Horvath *et al.*, 2008). As type-AB cyclones, it is characterized by the simultaneous presence of a large-scale cyclone, belonging to the same upper-level system, on its western side; however, it differs since the large-scale cyclone does not form over the Gulf of Genoa (it originates in the lee of the Atlas Mountains) and both cyclones do not move southeastward along the Tyrrhenian coast and the Adriatic Sea respectively (they move northward, driven by a southerly steering flow). Finally, like category C-II cyclones, the large-scale system does not originate over the Adriatic and over the Gulf of Genoa, but it differs since the small-scale pressure minimum detaches from the large-scale cyclone (the presence of two simultaneous cyclones is not contemplated in the C-II category).

Sensitivity experiments indicate that sea-surface fluxes were not important for the intensification of the cyclone. The secondary role played by the air–sea interaction processes and by convection indicate that the cyclone, even if it has a low-level warm core (its vertical extent can be estimated from 1,000 to about 650 hPa), shows very different dynamics compared with Mediterranean tropical-like cyclones or with intense Mediterranean extratropical cyclones partially sustained by intense convection (e.g., Vaia storm; Davolio *et al.*, 2020). Furthermore, the cyclone appears different from vortices in which the warm core is the result of seclusion of warm air (as described in Mazza *et al.*, 2017; Fita and Flaounas, 2018; Category B in the classification of Miglietta and Rotunno, 2019 or Group 3 in the classification of Dafis *et al.*, 2020); in fact, the cyclone develops at the southern tip of the warm and moist air tongue advected northward from the southern Mediterranean, several 100 km distant from the large-scale cyclone center, thus it is not associated with pre-existent baroclinic zones related to this larger-scale vortex. Some analogies can be found with Medicanes of Category C (Miglietta and Rotunno, 2019), such as the Ionian cyclone of September 2006 (Moscatello *et al.*, 2008b), which showed a similar extent of a few tens of km and underwent a strong intensification after its interaction with an upper-level PV streamer associated with a large-scale pressure minimum over the

Tyrrhenian Sea, as it moved near the left exit of a jet stream (Chaboureau *et al.*, 2012). However, in contrast to the latter, the present cyclone did not exhibit a deep warm core, but rather hybrid characteristics.

In conclusion, the present study re-affirms the existence of a continuum of cyclones between tropical and extratropical systems, showing how the complex orography and rough coastline of the Mediterranean basin make the range of possible characteristics of cyclones even wider compared to environments with more uniform morphology. As suggested in Garde *et al.* (2010), a strong effort should be put in the numerical exploration of the gray areas between these two categories of cyclones, especially considering that the region is highly responsive to climate change (Giorgi, 2006), and that the risk related to Mediterranean cyclones is expected to increase in the future (e.g., Romera *et al.*, 2017). This is especially true in the northern Adriatic, where a projected increase between 5 and 10 cm is expected in 100-year return times for Medicanes-induced coastal sea-surface elevations, with significant intermodel agreement (Toomey *et al.*, 2022). It is right along this line that the COST Action CA19109 “MedCyclones” has been trying to gather scientists of weather and climate, as well as the operational meteorological community, with the aim of improving our understanding of Mediterranean cyclones and attaining more accurate forecasts. The collaboration within the present research activity is a clear example of the powerful impact of sharing tools and expertise.

AUTHOR CONTRIBUTIONS

Mario Marcello Miglietta: Conceptualization; investigation; methodology; supervision; writing – original draft; writing – review and editing. **Federico Buscemi:** Data curation; investigation; visualization. **Stavros Dafis:** Data curation; investigation; resources; software; visualization. **Alvise Papa:** Data curation; funding acquisition. **Alessandro Tiesi:** Resources; software; visualization. **Dario Conte:** Software. **Silvio Davolio:** Conceptualization; writing – original draft; writing – review and editing. **Emmanouil Flaounas:** Resources; software; supervision. **Vincenzo Levizzani:** Methodology; supervision; writing – original draft. **Richard Rotunno:** Investigation; methodology; writing – original draft.

ACKNOWLEDGMENT

This work was supported by: the Technical-scientific Collaboration Agreement of CNR-ISAC with the Tide Forecast and Early Warning Center (CPSM)–Civil Protection–Municipality of Venice. The computational time was partially granted from the National Infrastructures for Research and Technology S.A. (GRNET S.A.) in

the Greek HPC facility–ARIS under project adapt2CC. This article is a contribution to the COST Action CA19109 “MedCyclones: European Network for Mediterranean Cyclones in weather and climate”. Open Access Funding provided by Consiglio Nazionale delle Ricerche within the CRUI-CARE Agreement.

FUNDING INFORMATION

Open Access Funding provided by Consiglio Nazionale delle Ricerche within the CRUI-CARE Agreement. The National Center for Atmospheric Research (NCAR) is sponsored by the National Science Foundation.

ORCID

Mario Marcello Miglietta  <https://orcid.org/0000-0003-2898-1595>

Stavros Dafis  <https://orcid.org/0000-0002-1513-1930>

Alvise Papa  <https://orcid.org/0000-0001-5979-9935>

Silvio Davolio  <https://orcid.org/0000-0001-8704-1814>

Vincenzo Levizzani  <https://orcid.org/0000-0002-7620-5235>

REFERENCES

- Alpert, P., Tsidulko, M. and Izigsohn, D. (1999) A shallow short-lived meso-beta cyclone over the Gulf of Antalya, eastern Mediterranean. *Tellus A*, 51, 249–262. <https://doi.org/10.3402/tellusa.v51i2.12319>.
- Bianco, A., Bonometto, A., Casaioli, M., Coraci, E., Cornello, M., Crosato, F., Ferla, M., Mariani, S., Morucci, S., Favaro, M., Massaro, G., Papa, A., Pastore, F., Sambo, E., Tosoni, A., Bajo, M., Cavaleri, L., Chiggiato, J., Ferrarin, C. and Umgiesser, G. (2020) Novembre 2019. Un mese di maree eccezionali. Dinamica e anomalie dell'evento del 12 novembre 2019. Dati, statistiche e analisi degli eventi. [A month of exceptional tides. Dynamics and anomalies of the event of November 12, 2019. Data, statistics and analysis of events]. Available at: https://www.comune.venezia.it/sites/comune.venezia.it/files/documenti/centro_maree/bibliografia/Novembre_2019_un_mese_di_maree_eccezionali-Dinamica_e_anomalia_dell'evento_del_12novembre.pdf (Accessed: March 18, 2022)
- Bosart, L.F. and Lackmann, G.M. (1995) Postlandfall tropical cyclone reintensification in a weakly baroclinic environment: a case study of hurricane David (September 1979). *Mon. Wea. Rev.*, 123, 3268–3291. [https://doi.org/10.1175/1520-0493\(1995\)123<3268:PTCRIA>2.0.CO;2](https://doi.org/10.1175/1520-0493(1995)123<3268:PTCRIA>2.0.CO;2).
- Brzović, N. (1999) Factors affecting the Adriatic cyclone and associated windstorms. *Contributions to Atmospheric Physics*, 72, 51–65.
- Buzzi, A. and Tibaldi, S. (1978) Cyclogenesis in the lee of the Alps: a case study. *Quart. J. Roy. Meteor. Soc.*, 104, 271–287. <https://doi.org/10.1002/qj.49710444004>.
- Buzzi, A., Davolio, S. and Fantini, M. (2020) Cyclogenesis in the lee of the Alps: a review of theories. *Bull. of Atmos. Sci. and Technol.*, 1, 433–457. <https://doi.org/10.1007/s42865-020-00021-6>.
- Campins, J., Jansà, A. and Genovés, A. (2006) Three-dimensional structure of western Mediterranean cyclones. *International Journal of Climatology*, 26, 323–343. <https://doi.org/10.1002/joc.1275>.
- Cavaleri, L., Bajo, M., Barbariol, F., Bastianini, M., Benetazzo, A., Bertotti, L., Chiggiato, J., Ferrarin, C., Trincardi, F. and Umgiesser, G. (2020) The 2019 flooding of Venice and its implications for future predictions. *Oceanography*, 33, 42–49. <https://doi.org/10.5670/oceanog.2020.105>.
- Cavicchia, L., von Storch, H. and Gualdi, S. (2014) A long-term climatology of medicanes. *Climate Dynamics*, 43, 1183–1195. <https://doi.org/10.1007/s00382-013-1893-7>.
- Chaboureaud, J.-P., Pantillon, F., Lambert, D., Richard, E. and Claud, C. (2012) Tropical transition of a Mediterranean storm by jet crossing. *Quart. J. Roy. Meteor. Soc.*, 138, 596–611. <https://doi.org/10.1002/qj.960>.
- Cioni, G., Cerrai, D. and Klocke, D. (2018) Investigating the predictability of a Mediterranean tropical-like cyclone using a storm-resolving model. *Quart. J. Roy. Meteor. Soc.*, 144, 1598–1610. <https://doi.org/10.1002/qj.3322>.
- Dafis, S., Claud, C., Kotroni, V., Lagouvardos, K. and Rysman, J.-F. (2020) Insight into convective evolution of Mediterranean tropical-like cyclones. *Quart. J. Roy. Meteor. Soc.*, 146, 4147–4169. <https://doi.org/10.1002/qj.3896>.
- Davolio, S., Volontè, A., Manzato, A., Pucillo, A., Cicogna, A. and Ferrario, M.E. (2016) Mechanisms producing different precipitation patterns over north-eastern Italy: insights from HyMeX-SOP1 and previous events. *Quart. J. Roy. Meteor. Soc.*, 142, 188–205. <https://doi.org/10.1002/qj.2731>.
- Davolio, S., Della Fera, S., Laviola, S., Miglietta, M.M. and Levizzani, V. (2020) Heavy precipitation over Italy from the Mediterranean storm “Vaia” in October 2018: assessing the role of an atmospheric river. *Mon. Wea. Rev.*, 148, 3571–3588. <https://doi.org/10.1175/MWR-D-20-0021.1>.
- Dudhia, J. (1989) Numerical study of convection observed during the winter monsoon experiment using a mesoscale two-dimensional model. *Journal of the Atmospheric Sciences*, 46, 3077–3107. [https://doi.org/10.1175/1520-0469\(1989\)046<3077:NSOCOD>2.0.CO;2](https://doi.org/10.1175/1520-0469(1989)046<3077:NSOCOD>2.0.CO;2).
- Emanuel, K. (2005) Genesis and maintenance of Mediterranean hurricanes. *Advances in Geosciences*, 2, 217–220. <https://doi.org/10.5194/adgeo-2-217-2005>.
- Ferrarin, C., Bajo, M., Benetazzo, A., Cavaleri, L., Chiggiato, J., Davison, S., Davolio, S., Lionello, P., Orlić, M. and Umgiesser, G. (2021) Local and large-scale controls of the exceptional Venice floods of November 2019. *Progr. Oceanography*, 197, 102628. <https://doi.org/10.1016/j.pocean.2021.102628>.
- Fink, A.H., Pohle, S., Pinto, J.G. and Knippertz, P. (2012) Diagnosing the influence of diabatic processes on the explosive deepening of extratropical cyclones. *Geophysical Research Letters*, 39, L07803. <https://doi.org/10.1029/2012GL051025>.
- Fita, L. and Flaounas, E. (2018) Medicanes as subtropical cyclones: the December 2005 case from the perspective of surface pressure tendency diagnostics and atmospheric water budget. *Quart. J. Roy. Meteor. Soc.*, 144, 1028–1044. <https://doi.org/10.1002/qj.3273>.
- Flaounas, E., Gray, S.L. and Teubler, F. (2021) A process-based anatomy of Mediterranean cyclones: from baroclinic lows to tropical-like systems. *Weather Clim. Dynam.*, 2, 255–279. <https://doi.org/10.5194/wcd-2-255-2021>.

- Flaounas, E., Davolio, S., Raveh-Rubin, S., Pantillon, F., Miglietta, M.M., Gaertner, M.A., Hatzaki, M., Homar, V., Khodayar, S., Korres, G., Kotroni, V., Kushta, J., Reale, M. and Ricard, D. (2022) Mediterranean cyclones: current knowledge and open questions on dynamics, prediction, climatology and impacts. *Wea. Clim. Dynam.*, 3, 173–208. <https://doi.org/10.5194/wcd-3-173-2022>.
- Garde, L.A., Pezza, A.B. and Bye, J.A.T. (2010) Tropical transition of the 2001 Australian duck. *Mon. Wea. Rev.*, 138, 2038–2057. <https://doi.org/10.1175/2009MWR3220.1>.
- Giorgi, F. (2006) Climate change hot-spots. *Geophysical Research Letters*, 33, L08707. <https://doi.org/10.1029/2006GL025734>.
- Hallerstig, M., Magnusson, L., Kolstad, E.W. and Mayer, S. (2021) How grid-spacing and convection representation affected the wind speed forecasts of four polar lows. *Quart. J. Roy. Meteor. Soc.*, 147, 150–165. <https://doi.org/10.1002/qj.3911>.
- Hong, S.-Y., Noh, Y. and Dudhia, J. (2006) A new vertical diffusion package with an explicit treatment of entrainment processes. *Mon. Wea. Rev.*, 134, 2318–2341. <https://doi.org/10.1175/MWR3199.1>.
- Horvath, K., Lin, Y.-L. and Ivančan-Picek, B. (2008) Classification of cyclone tracks over the Apennines and the Adriatic Sea. *Mon. Wea. Rev.*, 136, 2210–2227. <https://doi.org/10.1175/2007MWR2231.1>.
- IPCC. (2021) Climate change 2021: the physical science basis. In: Masson-Delmotte, V., Zhai, P., Pirani, A., Connors, S.L., Péan, C., Berger, S., Caud, N., Chen, Y., Goldfarb, L., Gomis, M.I., Huang, M., Leitzell, K., Lonnoy, E., Matthews, J.B.R., Maycock, T.K., Waterfield, T., Yelekçi, O., Yu, R. and Zhou, B. (Eds.) *Contribution of working group I to the sixth assessment report of the intergovernmental panel on climate change*. Cambridge: Cambridge university press.
- Kain, J.S. (2004) The Kain-Fritsch convective parameterization: an update. *Journal of Applied Meteorology*, 43, 170–181. [https://doi.org/10.1175/1520-0450\(2004\)043<0170:TKCPAU>2.0.CO;2](https://doi.org/10.1175/1520-0450(2004)043<0170:TKCPAU>2.0.CO;2).
- Maheras, P., Flocas, H.A., Patrikas, I. and Anagnostopoulou, C. (2001) A 40-year objective climatology of surface cyclones in the Mediterranean region: spatial and temporal distribution. *International Journal of Climatology*, 21, 109–130. <https://doi.org/10.1002/joc.599>.
- Manzato, A., Riva, V., Tiesi, A. and Miglietta, M.M. (2020) Analysis of the July 4, 2007 hailstorm in NE Italy. *Q. J. Roy. Meteor. Soc.*, 146, 3587–3611. <https://doi.org/10.1002/qj.3886>.
- Malguzzi, P., Grossi, G., Buzzi, A., Ranzi, R. and Buizza, R. (2006) The 1966 ‘century’ flood in Italy: a meteorological and hydrological revisit. *Journal of Geophysical Research*, 111, D24106. <https://doi.org/10.1029/2006JD007111>.
- Mazza, E., Ulbrich, U. and Klein, R. (2017) The tropical transition of the October 1996 Medicane in the Western Mediterranean Sea: a warm seclusion event. *Mon. Wea. Rev.*, 145, 2575–2595. <https://doi.org/10.1175/MWR-D-16-0474.1>.
- Miglietta, M.M., Moscatello, A., Conte, D., Mannarini, G., Lacorata, G. and Rotunno, R. (2011) Numerical analysis of a Mediterranean hurricane over South-Eastern Italy: sensitivity experiments to sea surface temperature. *Atmospheric Research*, 101, 412–426. <https://doi.org/10.1016/j.atmosres.2011.04.006>.
- Miglietta, M.M., Laviola, S., Malvaldi, A., Conte, D., Levizzani, V. and Price, C. (2013) Analysis of tropical-like cyclones over the Mediterranean Sea through a combined modelling and satellite approach. *Geophysical Research Letters*, 40, 2400–2405. <https://doi.org/10.1002/grl.50432>.
- Miglietta, M.M., Cerrai, D., Laviola, S., Cattani, E. and Levizzani, V. (2017) Potential vorticity patterns in Mediterranean “hurricanes”. *Geophysical Research Letters*, 44, 2537–2545. <https://doi.org/10.1002/2017GL072670>.
- Miglietta, M.M. (2019) Mediterranean tropical-like cyclones (Medicane). *Atmosphere*, 10, 206.
- Miglietta, M.M. and Rotunno, R. (2019) Development mechanisms for Mediterranean tropical-like cyclones (Medicane). *Quart. J. Roy. Meteor. Soc.*, 145, 1444–1460. <https://doi.org/10.1002/qj.3503>.
- Mlawer, E.J., Taubman, S.J., Brown, P.D., Iacono, M.J. and Clough, S.A. (1997) Radiative transfer for inhomogeneous atmosphere: RRTM, a validated correlated k-model for the longwave. *Journal of Geophysical Research*, 102, 16663–16682. <https://doi.org/10.1029/97JD00237>.
- Moscatello, A., Miglietta, M.M. and Rotunno, R. (2008a) Numerical analysis of a Mediterranean “hurricane” over southeastern Italy. *Mon. Wea. Rev.*, 136, 4373–4397. <https://doi.org/10.1175/2008MWR2512.1>.
- Moscatello, A., Miglietta, M.M. and Rotunno, R. (2008b) Observational analysis of a Mediterranean ‘hurricane’ over South-Eastern Italy. *Weather*, 63, 306–311. <https://doi.org/10.1002/wea.231>.
- Niu, G.-Y., Yang, Z.-L., Mitchell, K.E., Chen, F., Ek, M.B., Barlage, M., Kumar, A., Manning, K., Niyogi, D., Rosero, E., Tewari, M. and Xia, Y. (2011) The community Noah land surface model with multi parameterization options (Noah-MP): 1. Model description and evaluation with local-scale measurements. *Journal of Geophysical Research*, 116, D1210. <https://doi.org/10.1029/2010JD015139>.
- Noyelle, R., Ulbrich, U., Becker, N. and Meredith, E.P. (2019) Assessing the impact of sea surface temperatures on a simulated medicane using ensemble simulations. *Natural Hazards and Earth System Sciences*, 19, 941–955. <https://doi.org/10.5194/nhess-19-941-2019>.
- Petterssen, S. and Smebye, S.J. (1971) On the development of extratropical cyclones. *Quart. J. Roy. Meteor. Soc.*, 97, 457–482.
- Petterssen, S. (1936) Contribution to the theory of frontogenesis. *Geof. Pub.*, 11(6), 1–27.
- Portmann, R., González-Alemán, J.J., Sprenger, M. and Wernli, H. (2020) How an uncertain short-wave perturbation on the North Atlantic wave guide affects the forecast of an intense Mediterranean cyclone (Medicane Zorbas). *Wea. Clim. Dynam.*, 1, 597–615. <https://doi.org/10.5194/wcd-1-597-2020>.
- Pytharoulis, I. (2018) Analysis of a Mediterranean tropical-like cyclone and its sensitivity to the sea surface temperatures. *Atmospheric Research*, 208, 167–179. <https://doi.org/10.1016/j.atmosres.2017.08.009>.
- Rasmussen, E. and Zick, C. (1987) A subsynoptic vortex over the Mediterranean with some resemblance to polar lows. *Tellus A*, 39, 408–425. <https://doi.org/10.1111/j.1600-0870.1987.tb00318.x>.
- Ricchi, A., Miglietta, M.M., Bonaldo, D., Cioni, G., Rizza, U. and Carniel, S. (2019) Multi-physics ensemble versus atmosphere-ocean coupled model simulations for a tropical-like cyclone in the Mediterranean Sea. *Atmosphere*, 10(4), 202. <https://doi.org/10.3390/atmos10040202>.
- Romera, R., Sanchez, E., Dominguez, M., Gaertner, M.A. and Miglietta, M.M. (2017) Climate change projections of medicanes

- with a large multi-model ensemble of regional climate models. *Glob. Planet. Change*, 151, 134–143. <https://doi.org/10.1016/j.gloplacha.2016.10.008>.
- Rotunno, R. and Fantini, M. (1989) Petterssen's "type-B" cyclogenesis in terms of discrete, neutral eady modes. *Journal of the Atmospheric Sciences*, 46, 3599–3604. [https://doi.org/10.1175/1520-0469\(1989\)046<3599:PBITOD>2.0.CO;2](https://doi.org/10.1175/1520-0469(1989)046<3599:PBITOD>2.0.CO;2).
- Skamarock, W.C., Klemp, J.B., Dudhia, J., Gill, D.O., Liu, Z., Berner, J., Wang, W., Powers, J.G., Duda, M., Barker, D.M. and Huang, X.-Y. (2019) A Description of the Advanced Research WRF Model Version 4. No. NCAR/TN-556+STR. Boulder, CO: NCAR. <https://doi.org/10.5065/1dfh-6p97>.
- Stein, U. and Alpert, P. (1993) Factor separation in numerical simulations. *J. Atmos. Res.*, 50, 2107–2115.
- Thompson, G., Field, P.R., Rasmussen, R.M. and Hall, W.D. (2008) Explicit forecasts of winter precipitation using an improved bulk microphysics scheme. *Part II: Implementation of a new snow parameterization*. *Mon. Wea. Rev.*, 136, 5095–5115. <https://doi.org/10.1175/2008MWR2387.1>.
- Toomey, T., Amores, A., Marcos, M., Orfila, A. and Romero, R. (2022) Coastal hazards of tropical-like cyclones over the Mediterranean Sea. *J. Geophys. Res. - Oceans*, 127, e2021JC017964. <https://doi.org/10.1029/2021JC017964>.
- Trini Castelli, S., Bisignano, A., Donateo, A., Landi, T.C., Martano, P. and Malguzzi, P. (2020) Evaluation of the turbulence parametrization in the MOLOCH meteorological model. *Quart. J. Roy. Meteor. Soc.*, 146, 124–140. <https://doi.org/10.1002/qj.3661>.

How to cite this article: Miglietta, M.M., Buscemi, F., Dafis, S., Papa, A., Tiesi, A., Conte, D. *et al.* (2023) A high-impact meso-beta vortex in the Adriatic Sea. *Quarterly Journal of the Royal Meteorological Society*, 149(751), 637–656. Available from: <https://doi.org/10.1002/qj.4432>